N. Wainfan, W. C. Walker, and G. L. Weissler, J. Appl. Phys. **24**, 1318 (1953)

G. Wehner, J. Appl. Phys. **21**, 62 (1950)

J. Woods, Proc. Phys. Soc. London **B67**, 843 (1956)

G. A. Woolsey, R. M. Reynolds, and L. P. Clarke, Phys. Letters **25A**, 656 (1967)

In current practice, glow discharge processes are almost always driven by high frequency power supplies, usually in the megahertz range. Such discharges are in some ways quite similar to, and in other ways very different from, the dc discharges that were discussed in the previous chapter. In such systems there is no real cathode or anode since the net flow of charge to either electrode is zero, unlike the dc discharge, and there is no uniquely defined floating potential, either.

WHY USE RF?

Charging of Insulator Surfaces

It often occurs, e.g. in sputter deposition or plasma etching (q.v.), that we wish to cover an electrode with an electrically insulating material. But if we place this insulator-covered electrode in an independently sustained dc discharge, the surface of the insulator will behave in the same way as the electrically isolated probe that was discussed in Chapter 3, "Sheath Formation at a Floating Substrate": the surface will charge up to floating potential, so that the fluxes of ions and electrons to the surface become equal, regardless of the potential applied to the electrode backing the insulator. These ions and electrons recombine on the surface, thus relieving the insulator of any need to conduct current, which it couldn't do anyway.

With the magnitude of plasma density ($\sim 10^{10}/cm^3$) found in the dc glow discharge processes under discussion, the sheath voltages developed at insulating or other electrically isolated surfaces are quite small, usually no more than 10 or 20 volts, and this may not be adequate for many purposes. We can see the problem more clearly, and also the solution, by following the various stages that result if one attempts to use an insulating target as the cathode in a dc discharge (Figure 5-1). In an equivalent circuit of this configuration, both the insulator and the discharge can be regarded as capacitors. By definition, capacitance is stored charge divided by the voltage across the capacitor plates ($C = Q/V$) and initially both capacitors will be uncharged with zero volts across them. Since Q is propor-

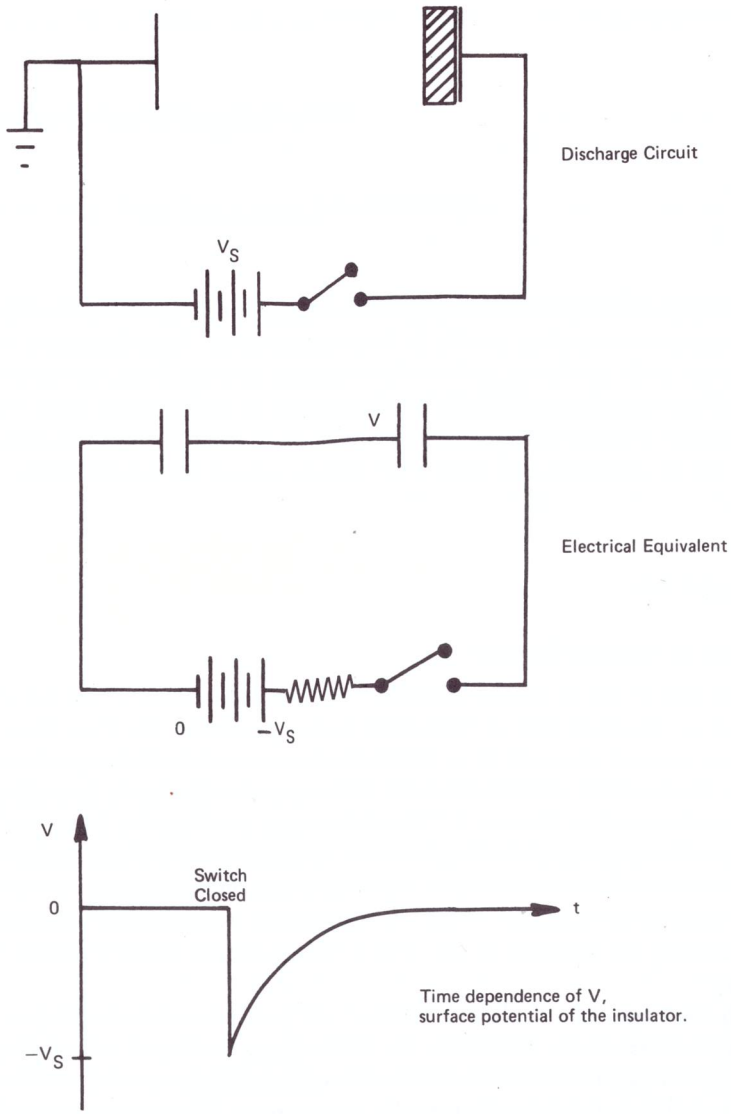

Figure 5-1. Surface charging of an insulating cathode

tional to V, and it takes time to change charge levels ($Q = \int i\,dt$), then the voltage across a capacitor cannot be changed instantaneously.

In our example (Figure 5-1), this means that both faces of the insulator will simultaneously drop to $-V_S$ volts when the switch is closed, V_S being the supply voltage. The glow discharge will be initiated and the negatively biased target will begin to be bombarded by positive ions. The insulator will start to charge positively (not because it collects the ions, but because it loses electrons as the ions are neutralized at its surface) and the potential V of the surface exposed to the discharge will rise towards zero (Figure 5-1). If the current to the target were proportional to V, then the potential rise would be exponential. Actually the current will not decrease proportionately as the sheath voltage decreases, so the form of the voltage rise will be more complex. But in either case, the discharge will be extinguished as soon as the insulator surface voltage drops below the discharge sustaining value.

The Use of AC Discharges

One proposal to deal with this problem was to use an ac discharge (Figure 5-2) so that the positive charge accumulated during one half-cycle can be neutralized by electron bombardment during the next half-cycle. Conventional mains frequency (50 Hz) was found to be not very effective because if the time during which the insulator charges up is much less than half the period of the ac supply, then most of the time the discharge will be off. Thus at low frequencies, there will be a series of short-lived discharges with the electrodes successively taking opposite polarities.

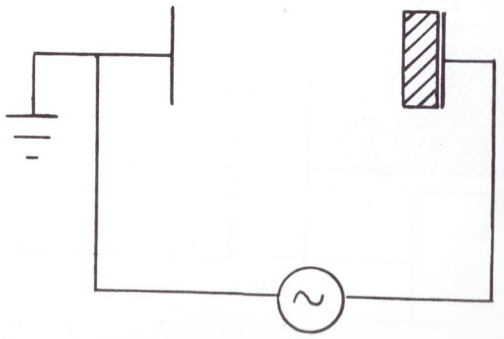

Figure 5-2. An ac glow discharge

Let's estimate the time it takes to charge up the insulator by considering the voltage rise across the capacitor in Figure 5-3. Although the current i to the target will actually decrease as the target charges up, it will be sufficient for an estimate to regard it as constant. Then the charge accumulated in t seconds will be $Q = it$, and so:

$$C = \frac{Q}{V} = \frac{it}{V}$$

and

$$t = \frac{CV}{i}$$

The capacitance of a piece of quartz 1/8" thick is about 1 pF/cm^2. Suppose that the applied voltage V is 1000 volts, and the ion current density is 1 mA/cm^2. (It's rather difficult to measure rf currents because of stray impedance effects at such high frequencies, and even if they could be measured accurately there would still be the problem of unravelling the ion current from the total rf current. However, by observing sputtering rates, we deduce that average rf ion currents are similar to dc sputtering currents, i.e. $\sim$ 1 mA/cm^2). These values give $t \sim 1\ \mu S$. This means that we can produce a discharge almost continuously at frequencies above about 1 MHz. Actually the insulator will not charge up so rapidly because the current will not be sustained at a constant value. In practice we can maintain a discharge quasi-continuously for frequencies above about 100 kHz. Wehner (1955) used a similar rationale in proposing rf discharges for sputtering purposes, and his proposals were successfully implemented some time later (Anderson et al. 1962).

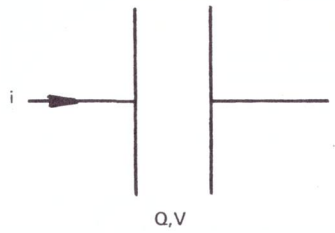

Figure 5-3. Charging of a capacitor

SELF-BIAS OF RF ELECTRODES

The simple argument just presented might suggest that ion bombardment of the insulator would occur for only half of each cycle at the most. Actually, nature is kinder than that and the much greater mobility of electrons in a discharge enables one to achieve almost continuous energetic ion bombardment if high enough frequencies are used. As we saw in Chapter 3, "Electron and Ion Temperatures", the acceleration f of a particle of mass m and charge e due to an electric field $\mathscr{E}$, is given by $f = \mathscr{E}\, e/m$, so that the lighter a particle is, the more it will accelerate due to a given force, and the greater the velocity it will acquire in a given time. But current is just the rate of flow of charge, and therefore depends on the velocity of the latter. So the lighter the charge is,

- the more current it will carry for a given electric field (the force), or
- the smaller field it will require to conduct a given current, or
- a combination of these.

In Chapter 3, we saw an effect of this behaviour: a biased probe immersed in a plasma can draw a large electron current but only a very much smaller ion current because of the much lower mean speed of the ions. This has a significant effect in rf discharges. Consider the glow discharge circuit shown in Figure 5-4, where C is the capacitance of an insulating target or is a blocking capacitor (the need for which will become apparent later) in the case of a conducting target. Let V_a be the (alternating) supply voltage, and let's see how the voltage V_b on

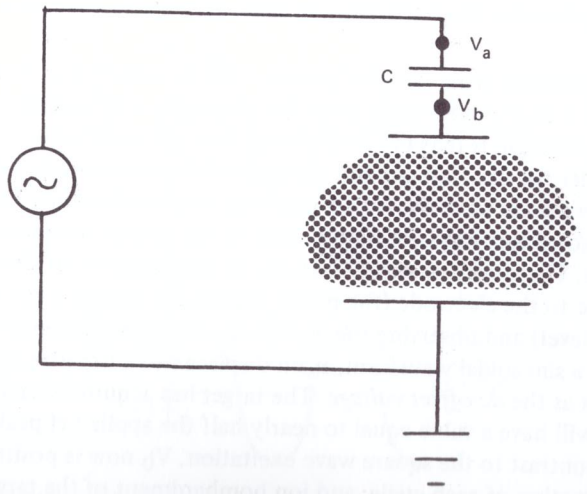

Figure 5-4. Schematic of a high frequency glow discharge circuit

the target surface varies. To simplify the argument, we'll assume that the plasma potential is close to zero (we'll see later when this assumption is justified; it wouldn't qualitatively change the argument anyway).

We begin by considering the application of a square wave power supply to the circuit (Chapman 1969). Let this have a peak-to-peak amplitude of 2 kV, so that V_a follows the form shown in Figure 5-5. The capacitor is initially uncharged, so that when V_a goes to -1 kV at time t = 0, then V_b takes the same value (the voltage across a capacitor cannot be instantaneously changed). The discharge is initiated, the target is bombarded by positive ions and the capacitor begins to charge positively (Figure 5-5) so that the target potential V_b rises towards zero. If the supply frequency is high enough, and in practice this turns out to be ~ 1 Mhz, then V_b will not have changed very much at the end of the half cycle, $\tau/2$; assume that it has risen to – 800V. At this instant V_a increases by 2 kV, and therefore so does V_b, in this case to + 1200 V. The positively charged target now draws a large electron current so that V_b decays towards zero much more rapidly than when subjected to ion bombardment. This is an example of the electron current being very much larger than the ion current for similar potential differences. Let's assume that V_b reaches + 100 V at the end of the first cycle (τ) and then as V_a switches, V_b will drop to - 1900 V and begin to rise. But since the ion current is small, V_b will not rise far before switching by + 2 kV again. After a few cycles, the voltage waveform will become repetitive with the main feature, apart from some distortion, that it has been dramatically displaced towards the negative, so that high energy ion bombardment of the target alternates with low energy electron bombardment. This is a manifestation of a much smaller potential being required for electrons than for ions, in order to conduct a given current.

The corresponding instantaneous current i will be something like that shown in Figure 5-5. I don't know quite what this waveform will look like; the principal requirement, though, is that the total charge flow per cycle sums to zero, so that the areas under the electron and ion portions of the current-time waveform must be equal. The square wave excitation was used only to illustrate the mechanism. The conventional sine wave excitation leads to the steady state waveforms shown in Figure 5-6. These voltage waveforms can be measured by attaching a high voltage probe to the electrode (the probe divides the voltage down to a safe and manageable level) and observing the waveform on a high frequency oscilloscope. V_b then has a sinusoidal waveform, again displaced to a negative value with a mean known as the *dc offset voltage*. The target has acquired a *self-bias*, which in this case will have a value equal to nearly half the applied rf peak-to-peak voltage. In contrast to the square wave excitation, V_b now is positive for only a very short fraction of each cycle, and ion bombardment of the target is almost continuous. As with the square wave, the charge flows during the positive and

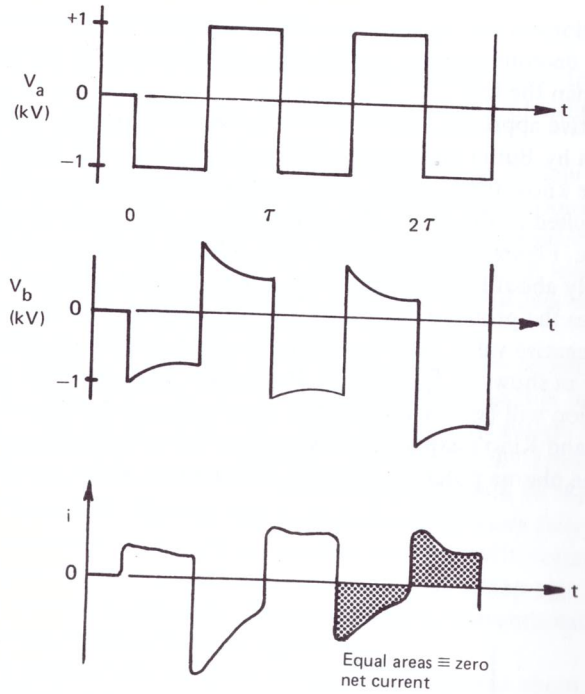

Figure 5-5. Voltage and target current waveforms when the circuit of Figure 5-4 is square wave excited

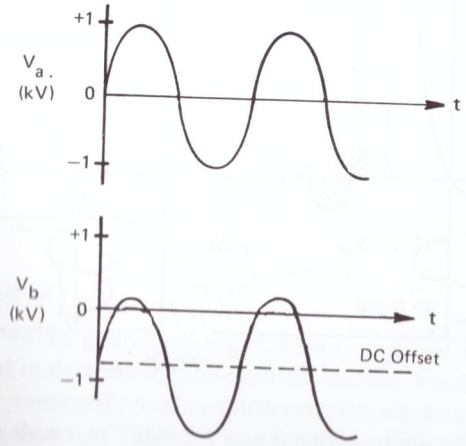

Figure 5-6. Voltage waveforms at generator (V_a) and target (V_b) in a conventional sinusoidally-excited rf discharge

negative portions of the V_b waveform must be equal and opposite; this time, the electrons demonstrate the combination of higher current and lower potential difference, than the ions.

An alternative approach to understanding the self-bias of an insulating electrode is given by Butler and Kino (1963) and is illustrated in Figure 5-7. From Chapter 3 we know that a probe at floating potential draws no net current. If a voltage is applied to the probe, the current drawn will be given by the probe characteristic. Figure 5-7a shows that when a probe is given an rf perturbation symmetrically about its initial potential, the asymmetry of the probe characteristic causes the probe to draw a net electron current. This charges the probe to a mean negative value with respect to floating potential, so as to draw a net zero current as shown in Figure 5-7b. In practical glow discharge processes, the rf perturbation will be very much larger than indicated in Figure 5-7. Additionally, Butler and Kino's experiments were made on a dc discharge; with an rf discharge the plasma potential has an rf perturbation which complicates the analysis.

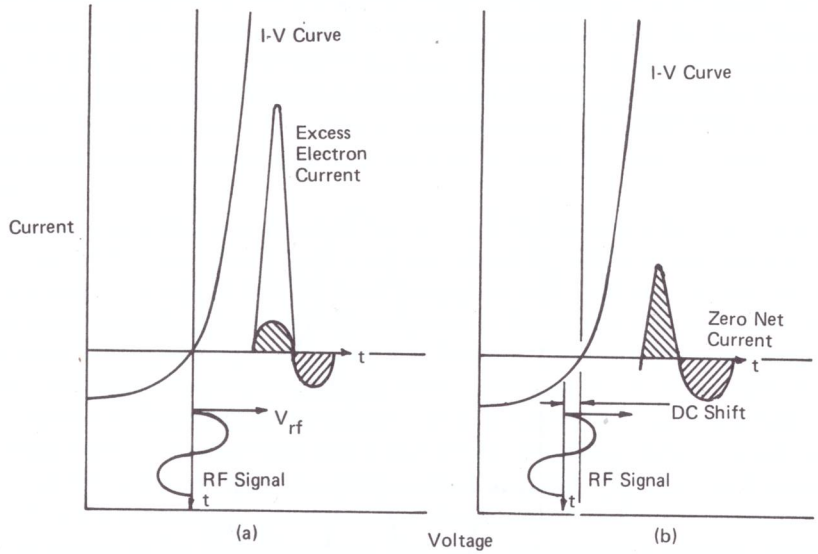

Figure 5-7. Self-biasing of a dielectric surface (Butler and Kino 1963)

THE EFFICIENCY OF RF DISCHARGES

As well as giving the ability to bombard insulating surfaces, it also transpires that the rf discharge is more efficient than its dc counterpart in promoting ionization and sustaining the discharge.

This can be shown by applying an ac source to a discharge. At low frequencies, this behaves like a double-ended dc discharge with similar limitations, particularly with regard to minimum operating pressure. But as the frequency increases, the minimum operating pressure begins to fall, reaching values of less than 1 mtorr at 13.56 MHz. There appears to be an additional mechanism occurring, or at least, an additional source of electron impact ionization.

Another manifestation of the same effect is that, for a given pressure, the impedance of a discharge decreases with increasing frequency, so that one can drive more current through the discharge with a given voltage. The system referred to in Chapter 4, "Architecture of the Discharge", with the V-I characteristics shown in Figure 4-1, has also been used as a dc sputtering system with an rf-induced substrate bias (Figure 5-8). The bias technique is described more fully in Chapter 6, and consists essentially of introducing another electrode with voltage (rf or dc) applied to it. Figure 5-8 shows how a comparatively small rf bias can increase the dc discharge current significantly. The *bias voltage* is conventionally taken as the dc offset voltage resulting from the applied rf.

Let us now ponder how this enhanced ionization might come about. Consider an electron oscillating along an x-axis in an ac field $\mathscr{E}$ of amplitude $\mathscr{E}_0$ and angular frequency ω:

$$\mathscr{E} = \mathscr{E}_0 \cos \omega t$$

Equation of electron motion is

$$m_e \ddot{x} = - e\mathscr{E}_0 \cos \omega t$$

and hence

$$\dot{x} = - \frac{e\mathscr{E}_0}{m_e \omega} \sin \omega t$$

and

$$x = \frac{e\mathscr{E}_0}{m_e \omega^2} \cos \omega t$$

The electron energy will be given by $\frac{1}{2} m_e \dot{x}^2$. Clearly the field strength and frequency are important in determining the electron motion. For the 13.56 MHz excitation frequency commonly used in sputtering, the electron amplitude and maximum energy are shown in Table 5-1 as a function of electric field strength. As we saw at the beginning of this chapter, the much greater mass of the ion will prevent it moving far in the rf field, or of acquiring much energy, compared with

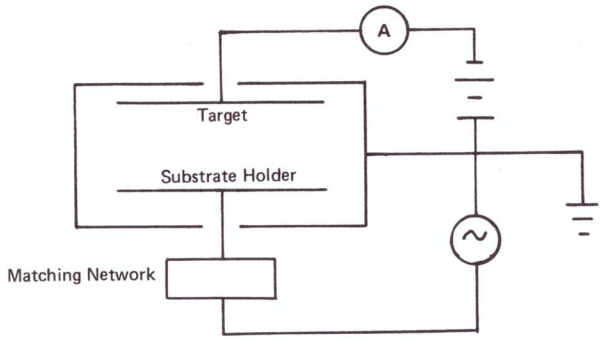

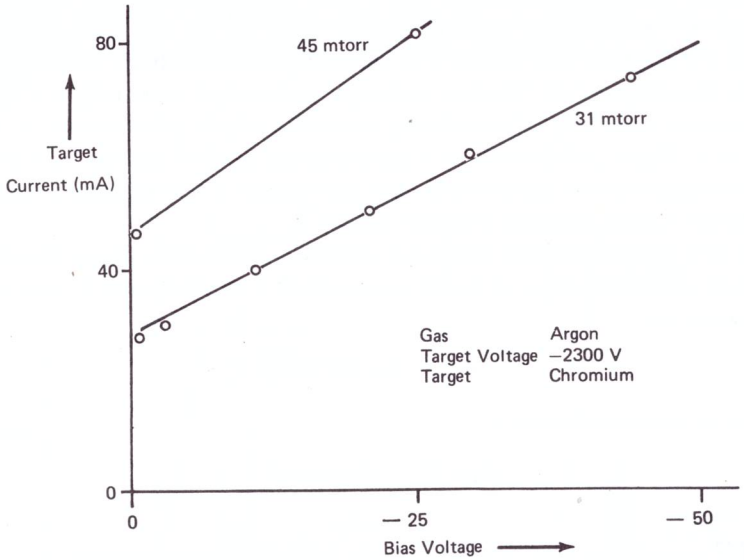

Figure 5-8. DC target current for a dc discharge in argon, vs. rf bias voltage on the substrate holder (Chapman 1975)

the electron. For an electron to acquire the 15.7 eV necessary to reach the ionization potential of argon, these values suggest that a minimum field strength somewhat above 10 V/cm would be required. However, from Figures 2-4 and 2-8 in Chapter 2, we know that the elastic collision cross-section of electrons around this energy is about 10^{-15} cm^2, whereas the ionization cross-section will be nearly two orders of magnitude smaller. This would suggest that much larger fields would be required. On the other hand, we know that the plasma will try

to reduce any applied field in a time determined by the plasma frequency to be around 1 nS, as discussed in Chapter 3. However, as discussed in many articles on high frequency discharges, for example by MacDonald and Tetenbaum (1978), if an electron makes an elastic collision at an appropriate time with respect to the phase of the electric field, then its velocity and energy would continue to increase. Ideally, the electron would make an elastic collision with an argon atom, reversing its motion at exactly the moment the field changed direction. In this way, electrons could reach ionizing energies for quite weak electric fields.

Table 5-1

Amplitude and maximum kinetic energy for an electron oscillating in an rf field without collisions

Field Strength (V/cm)	Amplitude (cm)	Velocity (cm/sec)	Energy (eV)
0.1	0.02 cm.	$2.1\ 10^6$	$1.13\ 10^{-3}$
1	0.24 cm.	$2.1\ 10^7$	0.11
10	2.42 cm.	$2.1\ 10^8$	11.3
100	24.2 cm.	$2.1\ 10^9$	1130
*1000	242 cm.	$2.1\ 10^{10}$	$1.13\ 10^5$

*ignoring relativistic effects

This mechanism seems to be accepted as the dominant ionization source in microwave discharges. At such frequencies, of the order of a few GHz (10^9 Hz), the amplitude of electron motion becomes quite small even for large fields. In addition, a large applied field can exist for a longer period before the plasma screens it out.

Such high frequencies are used in glow discharge processes, for example in the Toshiba microwave plasma etching system discussed in Chapter 7. However, we are mostly concerned in this book with excitation frequencies around 13 MHz. Koenig and Maissel (1970) and Maissel (1970) invoke this same mechanism to explain ionization in rf sputtering. But Holland et al. (1974), making similar calculations to those shown above, conclude that the secondary electrons which are emitted from the walls and target and are accelerated across the positive ion sheath into the plasma, act as an additional supply of electrons. In this case, electron collisions with the wall take the place of elastic collisions in the micro-

wave discharge. The explanation of Holland et al. is essentially that of the phenomenon of *multipacting*, which is discussed by MacDonald and Tetenbaum, and relies on secondary electron emission from the walls. If the electric field reverses at the right time, this can lead to efficient ionization; it can be a resonance phenomenon. MacDonald and Tetenbaum report the work of Hatch and Williams (1958); apparently the lower limit of the product of the frequency f and the electrode spacing d, for multipacting to occur, is 70 MHz cm. Many rf sputtering systems would be on this bottom end, but according to the predicted values, resonance would not occur until fd had a value of several hundred, for an rf peak to peak voltage of 1000 V.

Jackson (1970) also has discussed the conditions for rf sputtering discharge initiation and maintenance. He refers to the multipacting phenomenon, and also to the *electric field amplification* ideas of Vacquie et al. (1968) which also are based on secondary electron emission from the walls. Keller and Pennebaker (1979) reject the possibility of ionization by fast electrons from the target, and conclude that ionization is instead due to the large rf currents flowing through the glow or to electrons *surf riding* on the oscillating edge of the sheath. Apparently (Keller 1978) this surf riding effect, which must be distinguished from the analogy used to describe electron trapping in Chapter 4, relies on a result we derived in Chapter 1, "Energy Transfer in Binary Collisions": the rf field causes the electrode sheaths to grow and decay, modulating the sheath voltage and sheath length. So the sheath edge has an effective velocity v_w. An electron in the glow coming under the influence of the repulsive field at the edge of the moving sheath, would regard the encounter as a 'collision' with a massive particle. If the electron velocity perpendicular to the sheath edge is v_{el}, then by thinking in terms of relative velocity and using the result that a light particle striking a very heavy particle speeds away at twice the impact velocity, then we find that the velocity of the electron after impact is $v_{el} + 2v_w$ back into the glow; i.e. the electron has picked up energy from the oscillating sheath.

This result brings up another point. In Chapter 4, we saw that electrons tend to be trapped in the glow by the positive ion sheaths at the electrodes. In rf discharges, the effect is likely to be much larger. Although there are portions of the rf cycle when electrons can freely escape to the boundaries – in fact must do so to ensure zero net current – during most of the cycle the barrier to escape will be much larger than in dc discharges. This results from the larger plasma potentials generally extant in rf systems. Electron 'reflection' will occur at both target and counterelectrode sheaths, and will presumably be enhanced by Keller and Pennebaker's 'surf riding' effect at both sites.

So we have various possibilities for glow space ionization in rf discharges. But without clear experimental evidence, which is notably lacking for rf sputtering and plasma etching discharges, the detail of the process is not all clear. Unfortunately, although there have been many experiments on dc discharges and microwave discharges, the sputtering and etching discharges have received comparatively little attention. This is a frequent source of difficulty in trying to understand some of the strange effects that occur in 'our' discharges.

RF SHEATHS – COLLISIONS AND MODULATION

For sputtering purposes, in order to avoid gas phase scattering, rf systems are usually operated at the lower end of their operating range, from 1 mtorr up to about 40 mtorr. The dark space thickness is much less dependent on pressure than in the dc case, and is usually around 1 cm down to a pressure of a few mtorr, when it starts to increase. The comments in Chapter 4 about collision phenomena in dc sheaths being fairly independent of pressure apparently does not apply to rf sheaths.

Let's make some educated guesses about what happens in an rf sheath. Assume an argon pressure of 10 mtorr and a dark space length L of 1 cm. The probability of ionization for a secondary electron ejected from the target will be less than $nqL = (3.54\ 10^{14})(2.6\ 10^{-16})(1) = 0.09$, where we have used the maximum value of the ionization cross-section. However, the charge exchange cross-section is about a factor of 10 higher, giving a charge exchange probability of 1. So even at 10 mtorr, the sheath will not be collision-free, although there will not be any significant amount of ionization occurring there. So ionization is confined to the glow.

Although the lower frequency of collisions in the sheath will lead to less attenuation of the ion energy, the energy distribution of the ions will be considerably affected by the rf modulation of the sheath voltage and sheath thickness. A 500 eV argon ion has a velocity of $4.9\ 10^6$ cm/sec, which means that it would take 200 nS to travel 1 cm. But the period of a 13.56 MHz oscillation is 74 nS, and therefore the ion will undergo several oscillations on its way across the sheath.

There is a paper by Tsui (1968) which is frequently referred to. It considers the time-dependent ion and electron motions in an rf sheath, first to calculate the time-independent (dc offset) component of the sheath voltage, and then to calculate the energy distribution of ions at the cathode. Unfortunately the assumptions on which the analysis is based do not seem very realistic. It assumes that there are no collisions in the sheath over the range 2 – 20 mtorr, whereas there will be some charge exchange collisions, and that the electric field increases linearly across the sheath; this would seem to be even less acceptable at these dark space distance than in the Davis and Vanderslice (1963) analysis, although the high frequency dynamic sheath modulation makes this uncertain. The model also assumes that the ion velocity on entering the sheath is $n_i \overline{c_i}/4$,

although this is somewhat offset by the further assumption that $T_i \simeq T_e$. Finally it appears to treat the sheath thickness as a constant, and the plasma potential as constant and zero.

Coburn and Kay (1972) have made measurements of the energy distributions of various ions incident on a grounded electrode in an rf discharge. Their apparatus, which is conceptually the same as that used by Davis and Vanderslice, will be discussed further in Chapter 6. The sheath voltage at a grounded electrode should be numerically equal to the plasma potential. Therefore the energy of singly charged ions on the ground plane will be equivalent to the plasma potential, modulated by the rf component of the plasma potential, and attenuated by charge exchange collisions. Figure 5-9 shows the energy distributions of several ions at the ground plane, obtained by Coburn and Kay for a situation where the plasma potential was 100 V. Coburn and Kay quote several references to other relevant work and compare their results with a theoretical expression for the energy spread ΔE of the ion distribution, which predicts that $\Delta E \propto M^{-1/2}$, where M is the mass of the reterant ion. The basic rationale is that a fast light charged particle transits the sheath rapidly and responds to the instantaneous potential, whereas a heavy particle transits the sheath during several cycles and is aware only of the average potentials. This behavior is substantiated by the results of Figure 5-9, where the energy width of Eu^+ (molecular weight 151) is very narrow, whereas that of H_3^+ is very large. Measuring the distributions of a range of ionic species, they obtained reasonably good agreement with $\Delta E \propto M^{-1/2}$, although there were some problems near the origin.

For small sheath voltages, the thickness of the sheath is also quite small, thus minimizing charge exchange collisions. To obtain accurate values of V_p, Coburn and Kay used the energy distribution of Ar_2^+; compared with Ar^+, this has higher mass and hence lower ΔE, and a smaller charge exchange cross-section. Theory and experiment seem to be in comparatively good accord in this case.

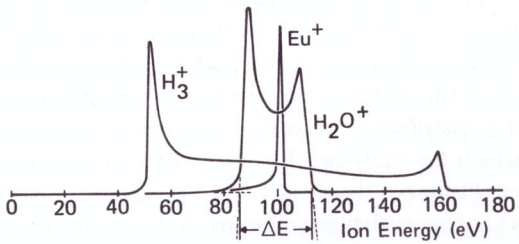

Figure 5-9. Energy distribution of H_3^+, H_2O^+, and Eu^+ at the substrate plans in a confined discharge. 13.56 MHz rf power = 100 W, argon pressure = 75 mTorr, target = 5-cm diam. (Coburn and Kay 1972)

MATCHING NETWORKS

It's common practice to use a matching network between the rf generator and the glow discharge (Figure 5-10). The purpose of this network is to increase the power dissipation in the discharge, and to protect the generator.

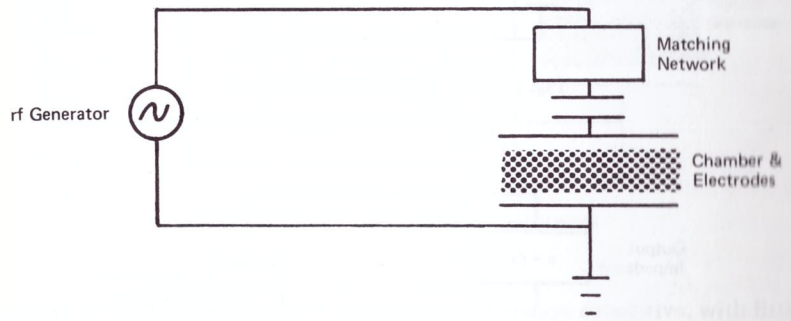

Figure 5-10. RF sputtering circuit with matching network

We can understand this better by considering the dc counterpart (Figure 5-11) in which a cell of emf E and internal resistance r is supplying power to an external load of variable resistance R. The current in the circuit is $E/(r+R)$ and therefore the power P dissipated in R is given by:

$$P = \frac{E^2 R}{(r+R)^2}$$

The power P will vary with the value of R. The maximum value of P is obtained by differentiation:

$$\frac{dP}{dR} = \frac{E^2(r+R)^2 - 2(r+R)E^2R}{(r+R)^2}$$

This differential has a zero value for R = r, which is for maximum P. Therefore to dissipate maximum power in a load, we match the resistance of the load to the resistance of the power supply.

There is an ac counterpart to this *dc maximum power theorem*. If the ac power supply in Figure 5-12 has an *internal* (also called *output*) *impedance* of a + jb ohms, then a similar calculus argument suggests that the impedance Z of the load must be equal to a - jb ohms (i.e. the conjugate of the generator output impedance) for maximum power transfer. The conjugate impedance is required so that the total load (internal plus external) is purely resistive. The equality of the resistive parts of source and load follows from the dc proof.

Figure 5-11. DC circuit with load R

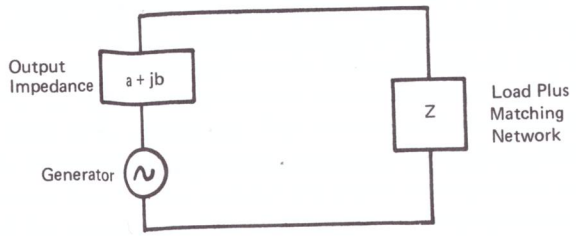

Figure 5-12. RF circuit with load impedance Z

In practice, to avoid large rf currents flowing round a circuit, generators are designed to have purely resistive outputs with a value that is usually 50 ohms. An rf discharge normally has a numerically larger and partly capacitive impedance which we cannot adjust without compromising the discharge process. We therefore simulate a load equal to the generator output impedance by combining the discharge load with a variable matching network load. The two loads will be reactive, and the matching network is therefore placed close to the discharge chamber so as to avoid power losses due to the large reactive currents flowing between these two components. A typical matching network configuration is shown in Figure 5-13.

Logan et al. (1969) have measured the impedance of an rf sputtering discharge in argon, and have employed the values obtained to design a matching network. Their technique was to use a matching network to tune their discharge to a generator of 50 Ω output impedance, and then to replace the generator with a 50 Ω load and measure the input impedance of the matching network (as seen from the discharge end) for the same dial settings. The value obtained should be the conjugate of the discharge impedance. This also follows from the maximum power theorem.

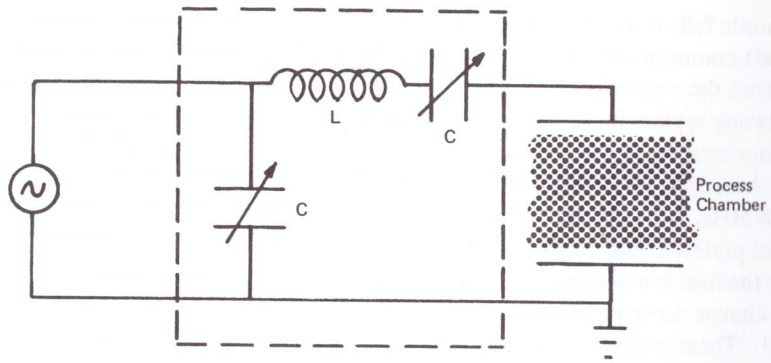

Figure 5-13. A typical rf matching network

Logan et al. found that the glow impedance was always capacitive, with little apparent dependence on power level (although there was some conflicting evidence on this point). The capacitance values (of a parallel capacitor-resistor representation) ranged from 0.08 pF/cm^2 at 5 mtorr to 0.12 pF/cm^2 at 20 mtorr, but increased at both pressures up to a value of 0.25 pF/cm^2 with an axial magnetic field of 150 gauss; 0.1 pF is equivalent to 1.2 10^5 Ω at 13.56 MHz. The parallel conductance ranged from 1.4 micromhos/cm^2 (i.e. the reciprocal of 7 10^5 Ω for each cm^2, presumably of the target in this case) at 5 millitorr up to 1.8 μmhos/cm^2 at 20 mtorr, and then increased with magnetic field up to values of around 4 μmhos/cm^2 at 150 gauss.

It is a condition of this analysis that the power losses in the matching network should be small, and unfortunately this is unlikely to have been the case. However, a design exercise based on the impedance values obtained gave good agreement between calculated and empirically found values of the matching network components.

WHY 13.56 MHz?

Many rf glow discharge processes operate at 13.56 MHz. There is nothing 'magic' about this number as far as the glow discharge is concerned. It just happens to be a frequency allotted by international communications authorities at which one can radiate a certain amount of energy without interfering with communications. Unfortunately this isn't such a great help for rf glow discharge systems because the glow discharge has so many nonlinear effects that it generates many harmonics of the fundamental frequency, and the radiation requirements on the harmonic frequencies are far more stringent. The sixth

harmonic falls in the VHF broadcast band, and the seventh and eighth fall in aircraft communication bands. At the Allen Clark Research Centre in Northampton, the converted 'hot dog' machine with which we powered an early rf sputtering system incapacitated the internal radio paging system. So it goes.

There seem to be two schools of thought regarding operating frequencies. One school restricts itself to the magic 13.56 MHz or to multiples at 27.12 MHz and 40.68 MHz, with the oscillator crystal-controlled at this frequency. The smaller school prefers to use frequencies that can be chosen to optimize performance; usually the load is made part of the oscillator circuit so that the operating frequency may change during a process (Jackson 1970, Vossen and O'Neill 1975, McDowell 1969). These systems tend to have greater stability as they remain 'tuned' over a broader range of operating parameters, i.e. they have a lower Q, and are less susceptible to damage when running untuned; however they do require more careful coupling and shielding. Their stability advantage is also somewhat offset now by the availability of improving automatic tuning systems.

VOLTAGE DISTRIBUTION IN RF SYSTEMS

In the first part of this chapter, in illustrating the action of an rf discharge, we made the assumption that the plasma potential was close to zero. This is relatively true for most sputter deposition systems, but quite untrue for other systems, such as a high pressure parallel plate plasma etcher.

The 'classical' treatment of voltage division in an rf discharge is by Koenig and Maissel (1970) and Koenig (1972). They considered the relationship between the unequal areas A_1 and A_2 of two electrodes, and the sheath voltages and thicknesses V_1 and V_2, D_1 and D_2 respectively, developed at the electrodes due to an rf discharge. If we make the assumption that the glow is equipotential, then the configuration of Figure 5-14 would suggest that $V_1 = V_2$ since these are the only dc voltages in the system and must therefore be equal and opposite. However, a blocking capacitor (Figure 5-15) changes that situation and is commonly used in glow discharge systems just to create asymmetry. Koenig and Maissel treat this situation by making the following assumptions:

1. That positive ions of mass m_i come from the glow space and traverse the dark spaces without making collisions, and with a space charge limited flux j_i:

$$j_i = \frac{KV^{3/2}}{m_i^{1/2}D^2}$$

where K is a constant.

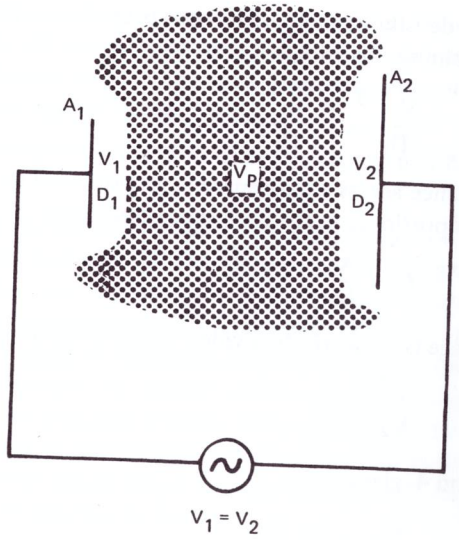

Figure 5-14. Voltage distribution – without blocking capacitor

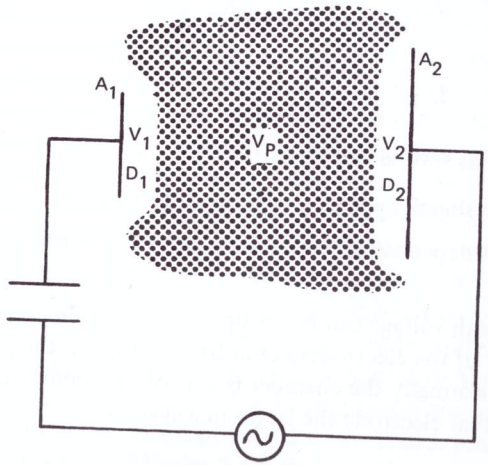

Figure 5-15. Voltage distribution – with blocking capacitor

2. That the current density of the positive ions is uniform and is equal at both electrodes. Combining this with 1.,

$$\frac{V_1^{3/2}}{D_1^{2}} = \frac{V_2^{3/2}}{D_2^{2}}$$

3. That the capacitance across a dark space is proportional to the electrode area and inversely proportional to the dark space thickness:

$$C \propto \frac{A}{D}$$

4. That the rf voltage is capacitively divided between the two sheaths:

$$\frac{V_1}{V_2} = \frac{C_2}{C_1}$$

combining 3. and 4. gives:

$$\frac{V_1}{V_2} = \frac{A_2}{D_2}\,\frac{D_1}{A_1}$$

and substituting this into 2.,

$$\frac{V_1^{3/2}}{V_2^{3/2}} = \frac{D_1^{2}}{D_2^{2}} = \left(\frac{A_1}{A_2}\,\frac{V_1}{V_2}\right)^2$$

$$\therefore \frac{V_1}{V_2} = \left(\frac{A_2}{A_1}\right)^4$$

This result suggests several things:

- The larger voltage sheath appears at the smaller electrode
- The fourth power dependence exaggerates the effect of geometrically asymmetric systems.
- A substantial sheath voltage can be set up at an electrode even when it is grounded. Either of the electrodes could be grounded in the preceding example, although normally the chamber is part of the grounded electrode and helps make that electrode the larger in a system.

Generalization of the Koenig Model

The area ratio model for sheath voltage distribution was developed for rf sputtering systems operating at a few mtorr. Three problems occur in its application, particularly at higher pressures:

a. The glow density can vary considerably throughout the volume of a system and sometimes will be confined essentially only between the electrodes. So there is a difference between the total geometric areas of the electrodes, and the areas as they appear to the plasma.

b. The assumption that the ion current density is equal at both electrodes is questionable.

c. The version of the Child-Langmuir used in the derivation is for a collisionless sheath where the ions free-fall (see Chapter 4). This is generally untrue in rf sheaths except at very low pressures ~ 1 mtorr or perhaps a little higher if change transfer does not impede ion motion. At higher pressures, one should use a mobility-limited or ionization-limited version of the space charge equation. For example, the former would suggest a voltage division varying as the cube of the area ratio if other assumptions remained unchanged. However, the existence of collisions in the sheath implies power absorption there, so that the sheaths can no longer be regarded as purely capacitive, and the equivalent circuit also has to change.

Experimental Test of the Voltage Distribution Model

Coburn and Kay (1972) have measured the relationships between target and substrate sheath voltages in a rf diode system operating at 13.56 MHz, as a function of area ratio. The plasma potential V_p was measured by the energy analysis technique mentioned in "RF Sheaths – Collisions and Modulation".

The area ratio was changed by using a series of pyrex confining cylinders of equal height and a range of radii. (Figure 5-16). A parameter R was defined as the ratio of the carbon target area to the total area of all other surfaces in contact with the plasma. This is not strictly the situation addressed by Koenig and Maissel, since the pyrex cylinder is insulating and therefore not part of the second (grounded) electrode. Coburn and Kay plotted the results they obtained for the substrate sheath voltage against the target sheath voltage $V_p - V_t$, and obtained a family of straight lines for different values of R (Figure 5-17).

The Koenig model predicts that the ratio of substrate to target voltage should be constant for given area ratio, and this appears to be well substantiated by the linear results of Figure 5-17, although the lines appear to have a common intercept which is not at the origin. The Koenig model also predicts that the sheath voltage ratio should be proportional to the fourth power of the inverse area ratio. In the context of Figure 5-17, that would translate into the slope (sheath voltage ratio) being proportional to R (the inverse area ratio) to the fourth power. In fact, the values obtained by Coburn and Kay suggest that the power dependence should be much closer to unity rather than the fourth power (Table 5-2). The reason for this disagreement is not at all clear. Although the

range of area ratios tested was quite small, and could not be considered an exhaustive test, the magnitude of disagreement is striking. The plasma potentials obtained are much larger than predicted; for example $V_p - V_t = 300$ V and $R = 0.289$ should give $V_p = 2.1$ V compared with an actual value of 101 V. These values are for the smallest containing cylinder, when the plasma should have been most aware of the wall and probably most uniform.

The overall conclusion seems to be that although the target and substrate sheath voltages are linearly dependent, and their ratio dependent on the inverse area ratio of their electrodes, both as predicted, there is some doubt about the power of the dependence.

Application to Sputtering and Reactive Ion Etching Systems

In a sputter deposition or etching system (Chapter 6), we want sputtering to be confined to specific electrodes. We do not want wall materials to be sputtered since these will act as contamination sources in a sputter deposited film. We therefore prefer to keep wall sheaths down to about 20 volts, which is a typical threshold for sputtering. This is achieved by making the target area much smaller than the wall area, with the resultant voltage division we saw previously.

Reactive ion etching systems (Chapter 7) are almost identical to sputtering systems, and the same rationale applies. This virtually guarantees electrode material being sputtered and backscattered onto the substrates, so compatible materials must be used.

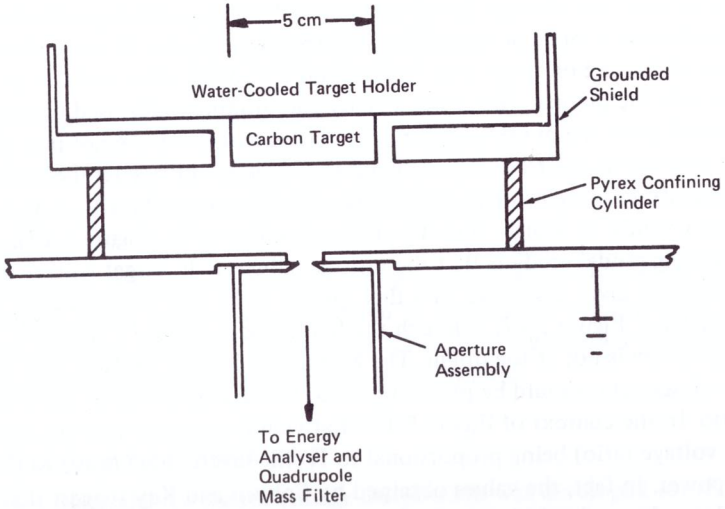

Figure 5-16. Chamber configuration for the area ratio experiments of Coburn and Kay (1972)

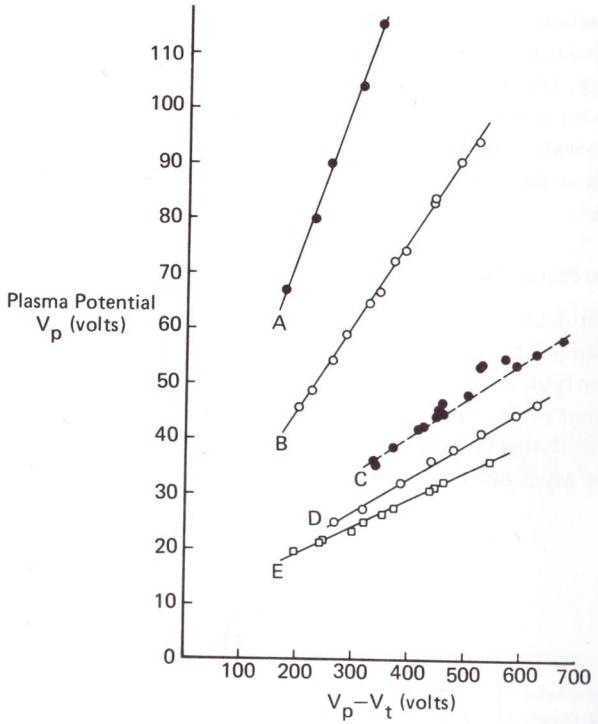

Figure 5-17. Plasma potential V_p vs. the dc voltage across the target-plasma sheath ($V_p - V_t$) for the five confining cylinders; argon pressure = 50 mtorr; interelectrode spacing = 1.88 cm. Curve A: R = 0.289, slope = 0.298; B: R = 0.208, slope 0.160; C: R = 0.142, slope ~ 0.07; D: R = 0.114, slope = 0.06; E: R = 0.092, slope = 0.05 (Coburn and Kay 1972)

Table 5-2

The power dependence y of the sheath voltage ratio on the inverse electrode area ratio, i.e. $V_1/V_2 = (A_2/A_1)^y$, as suggested by the results of Coburn and Kay (1972) shown in Figure 5-17.

Line	A	B	C	D	E
Slope	0.298	0.160	~0.07	0.063	0.052
Area Ratio	0.289	0.208	0.142	0.114	0.092
Power Dependence	0.98	1.17	~1.4	1.3	1.2

There is a tendency with these systems to make the target (sputtering) or wafer electrode (reactive ion etching) larger and larger so as to increase the system capacity. This reduces the area ratio of the electrodes so that the wall sheath voltage increases and sputtering inevitably results (Bresnock 1979) – contaminating the wafer surfaces. Microcircuits are extremely sensitive to certain materials, such as fast-diffusing metals – Cu, Fe, and Ni; quite tiny amounts can ruin devices.

Application to Planar Diode Reactors

In Chapter 7 on plasma etching, I have described a type of plasma reactor, often known as a *planar diode reactor*, which is used for etching and deposition. This type of reactor typically has two large electrodes of equal area, one grounded, inside a chamber of not-much-larger internal diameter; the chamber may be grounded or insulating (Figure 5-18). This configuration approaches the other extreme to the asymmetric sputtering system.

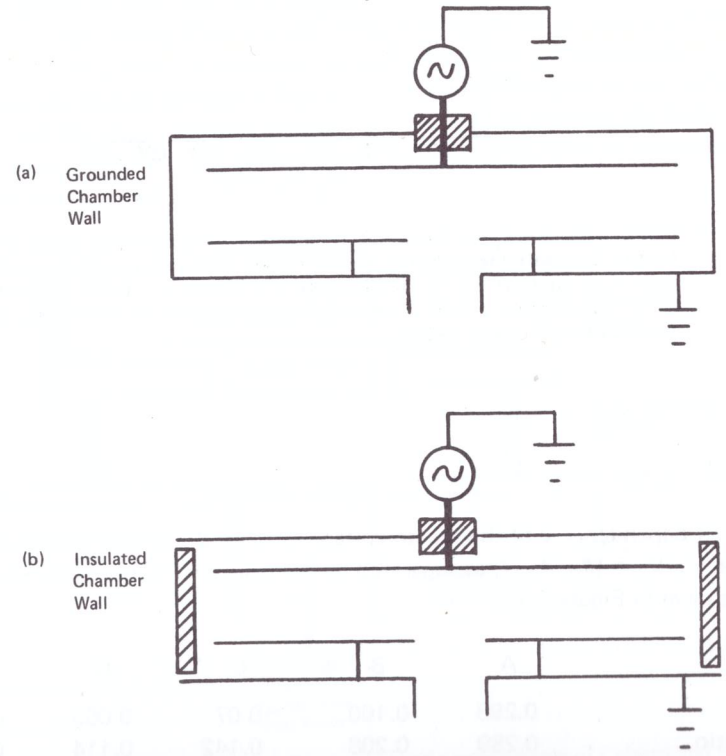

Figure 5-18. Planar diode reactors for deposition and etching

In these planar diodes, the wafer is placed on the grounded electrode. This appears to have caused some confusion and has mistakenly led some people to believe that only low energy ion bombardment can occur there. The Koenig model described earlier makes it clear that sheath voltages, and hence ion energies, can be quite substantial at a grounded wafer in such systems. The higher pressures (typically 500 mtorr) used might seem to ensure low ion energies due to the large number of collisions per unit length of travel, even though the sheath voltage is substantial. However, the sheaths at the electrodes are extremely thin at such high pressures, so that the total number of collisions attenuating the ion energies might not be so different from the low pressure case. Indeed we need quite substantial ion energies to explain directional plasma etching (q.v.) in such systems.

There are considerable advantages to being able to place wafers on a grounded electrode. However, we must recognize that it is easy to sputter material from both electrodes and from the wall, if too much power is applied. Vossen (1979) has identified aluminium contamination in a planar diode.

SYMMETRICAL SYSTEMS

It is interesting to look at this type of system in rather more detail, to get some idea of the sheath voltages involved. Consider the truly symmetrical system in Figure 5-19. The system retains its electrical symmetry regardless of the position of the matching network and regardless of the position of the system ground – both of which the discharge would be unaware of. Assume that the bottom electrode is well grounded (and this is a non-trivial matter because connecting wires can easily have a considerable impedance at radio frequencies). Let the (time dependent) voltage on the top electrode be V_{rf} (Figure 5-19). Let the two sheath voltages, which will be equal in magnitude (the symmetry demands that) although not in phase, be V_s and V_s' as shown, measured from their respective electrodes; each will have a dc component and an rf component, and the two rf components will be 180° out of phase as the sheaths alternate. So V_{rf} will not have a dc component, as expected for a symmetrical system, and can be represented by

$$V_{rf} = V_{rfo} \sin \omega t$$

as shown in Figure 5-20. If we assume that the glow is equipotential and of value V_p, then we also have

$$V_s = V_p - O$$

$$V_s' = V_p - V_{rf}$$

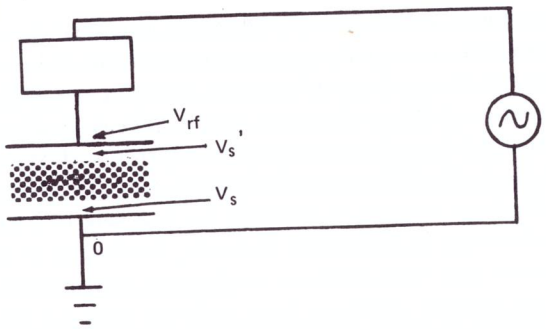

Figure 5-19. Schematic of a symmetrical rf system. $|V_s| = |V_s'|$

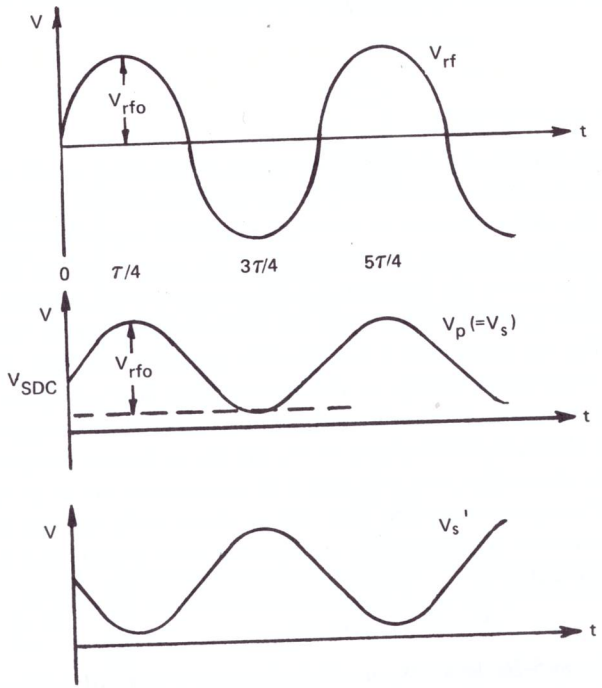

Figure 5-20. Sheath and electrode voltages in a symmetrical system
(a) Electrode voltage $V_{rfo} \sin \omega t$
(b) Sheath voltage V_s = plasma potential $V_p = V_{SDC} + \frac{1}{2}V_{rfo} \sin \omega t$
(c) Sheath voltages $V_s' = V_{SDC} + \frac{1}{2}V_{rfo} \sin(\omega t + \pi)$

The symmetry of the situation requires that V_p must exceed the potential V_{rfo} of the upper electrode at $\tau/4$ (τ = period) by exactly as much as it exceeds the potential of the lower electrode (OV) at $3\tau/4$. So the amplitude of V_p, and hence of V_s and V_s', must be exactly half of that of the applied rf in this symmetrical system, as shown in Figure 5-20, with a positive dc offset of V_{SDC}. This offset will be approximately equal to $V_{rfo}/2$; its precise magnitude will be determined by the electron current required during the portions of the cycle when V_p is close to the potential of either electrode.

The waveform of V_p is uncertain; a sinusoidal function has been assumed in Figure 5-20.

From the symmetry of the system, it is clear that the sheath voltage is just as large at the grounded electrode as at the ungrounded electrode. This is a very important point, and would apply just as well to a symmetrical system with insulated electrodes. We therefore have a clear distinction between the dc and rf cases. In the dc case, an insulator would charge up to floating potential (see Chapter 4) so that the sheath voltage was just a few volts. In the rf case, the sheath voltage at the insulator can be very substantial. It doesn't matter whether the plasma potential V_p is substantially dc and the potential of an electrode backing the insulator is rf powered, as in the example ("Self-Bias of RF Electrodes") earlier in the chapter; or whether the backing electrode is grounded and the plasma has a substantial modulation, as in the present example.

To illustrate the point further, we could build an assymmetric system for sputtering purposes, rather like a conventional system except that the insulating target would be grounded instead of the walls (Figure 5-21); provided that the target area is smaller than the wall area, the larger sheath voltage will still be developed at the target, regardless of the position of the electrical ground.

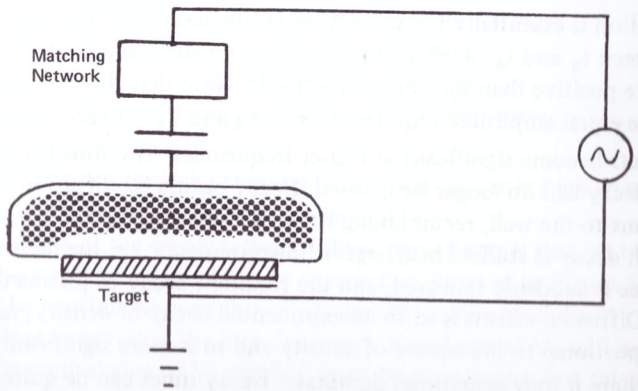

Figure 5-21. RF sputtering system with grounded target

Hence my comment at the beginning of the chapter that there is no uniquely defined floating potential in an rf system. Although it is generally accepted that an insulator backed by a conducting rf powered electrode will not charge up to floating potential (otherwise sputtering of insulators would not work!), it is not generally realized that an insulator backed by a grounded conducting electrode is in qualitatively the same situation if the plasma potential has an rf modulation. The magnitude of the modulation is important, of course. It may well be that the asymmetry of a conventional sputtering system results in a small enough plasma potential modulation that raising the plasma potential without changing the modulation does not increase the ion bombardment energy on an electrically isolated substrate, as observed by Coburn and Kay (1972), but this is generally untrue and particularly untrue for the symmetrical system.

Let's return to the symmetrical system and re-examine the assumption that all waveforms were sinusoidal (Figure 5-20). In this case the mean values of V_p, V_s, and V_s' would be equal to $V_{rfo}/2$ plus the minimum amount by which V_p exceeds zero (at $t = 3\tau/4$ in Figure 5-20). This minimum amount could be negative, but is unlikely to be significantly different from zero. So the plasma potential will be closely equal to $V_{rfo}/2$, or one quarter the rf peak-to-peak voltage.

But will the plasma potential waveform be sinusoidal? Let's consider, in Figure 5-22a, what will happen to the plasma potential V_p in a low frequency ac discharge, which is just like a double ended dc discharge. Initially ($t = 0$) there is no discharge and $V_p = 0$. As V_{rf} increases, it will reach, at t_1, a large enough value to initiate the discharge and V_p will rise to become a little more positive than V_{rf}. This continues until t_2 when V_{rf} is no longer large enough to sustain the plasma, and V_p drops to zero. At low enough frequencies, the times for establishment and extinction of the discharge will be negligibly small, so that V_p will change comparatively instantaneously.

The situation is essentially the same through the next half-cycle; the discharge exists between t_3 and t_4, during which time V_p remains just above OV, i.e. a little more positive than the counterelectrode. Note that this waveform for V_p satisfies the equal amplitude requirements of V_s and V_s' (Figure 5-19).

Two effects become significant at higher frequencies. The time for the discharge to decay can no longer be ignored. Decay occurs by diffusion of ions and electrons to the wall, recombining there, and by recombination in the gas phase. Such decay is studied in *afterglow* measurements; i.e. the discharge driving force is suddenly removed, and the resultant decay of plasma density is observed. Diffusion effects lead to an exponential decay of density; recombination is proportional to the square of density and so is more significant at higher densities where it may sometimes dominate. Decay times can be quite significant and are probably of the order of 1 msec for a sputtering discharge.

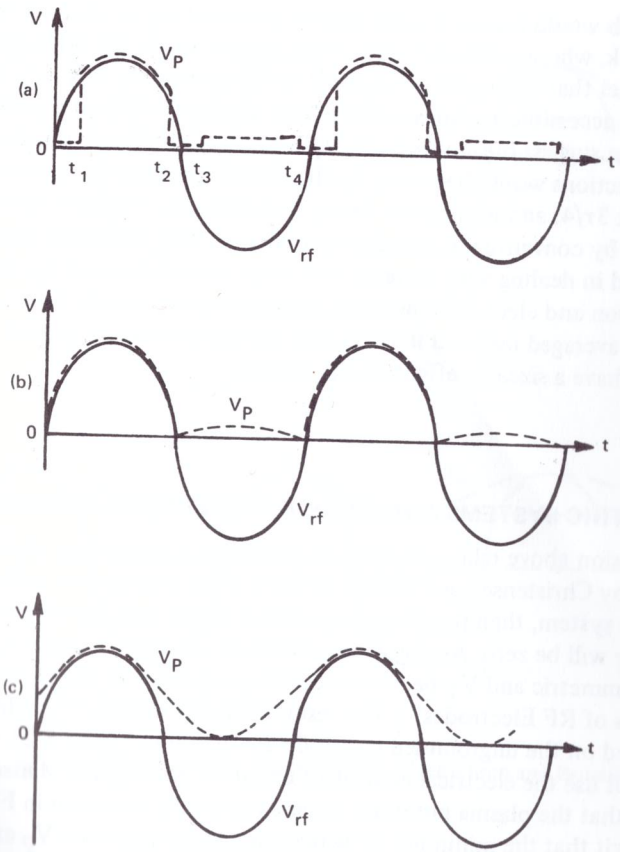

Figure 5-22. Voltage-time dependence in rf systems
(a) Low frequency discharge
(b) High frequency discharge?
(c) Assuming sinusoidal dependence

The second effect is the enhanced ionization that occurs in high frequency discharges, an effect we have already discussed.

The implication of the combination of these two effects is that, at high frequencies, there will be no initiation or destruction times as in Figure 5-22a; the plasma will be continuous even though its density will be modulated.

It is not clear to me what the high frequency waveform of V_p will be. Certainly the equivalence of V_s and V_s' must be maintained, but this can be achieved with many waveforms. I'm not sure whether the waveform should look like Figure 5-22b or like 5-22c. Perhaps someone else can help. It matters because

Figure 5-22b would lead to a mean plasma potential V_p of about ¼ the rf peak-to-peak, whereas Figure 5-22c would suggest about 1/8 peak-to-peak. One would expect that this could be resolved by measuring V_p, but only the mean is currently accessible and measurements by Vossen (1979) on a quasi-symmetrical system suggest mean values for V_p higher than either of the above. The above predictions would be wrong by the extent to which V_p exceeds ground potential at $3\tau/4$, and we may be wrong to ignore this. Vossen's measurements were made by conventional probe measurements. This technique must be re-evaluated in dealing with systems with large modulations of V_p; the nonlinear effects on ion and electron flow make it dangerous to assume that modulation of V_p will be averaged out, and it seems that the capacitance to ground of the probe will have a sizeable effect on the results.

ASYMMETRIC SYSTEMS AND MEASUREMENT OF PLASMA POTENTIAL

The discussion above relates directly to a method of measuring plasma potential proposed by Christensen and Brunot (1973). If we measure the voltage V_{rf} in a symmetric system, then it will be symmetrical about zero, and the mean target voltage V_T will be zero. As the system becomes asymmetric, then V_{rf} also becomes asymmetric and V_T becomes negative, as we saw in the earlier example ("Self-Bias of RF Electrodes"). The resultant waveforms for V_{rf} which would be observed on the ungrounded electrode are shown in Figure 5-23. Christensen and Brunot use the electrical equivalent circuit of Koenig and Maissel (1970) to conclude that the plasma potential varies sinusoidally as shown in Figure 5-23. It is implicit that the minimum by which the plasma potential V_p exceeds the electrode potential is negligible at certain points ($\tau/4$, $3\tau/4$) during the cycle, and that when insulating targets are used, the voltage drop across them is also negligible. The latter assumption is questionable.

If the mean target voltage is V, then Figure 5-23 predicts that the mean plasma potential will be given by:

$$\overline{V_p} = \frac{V_{rfo} + V_T}{2}$$

This gives an alternative to probes for the measurement of plasma potential and requires only an oscilloscope to observe the target waveform, or, as Christensen and Brunot propose, electronic techniques to automatically measure V_{rfo} and V_T, and hence calculate V_p; they report good agreement between this technique and conventional probe measurements.

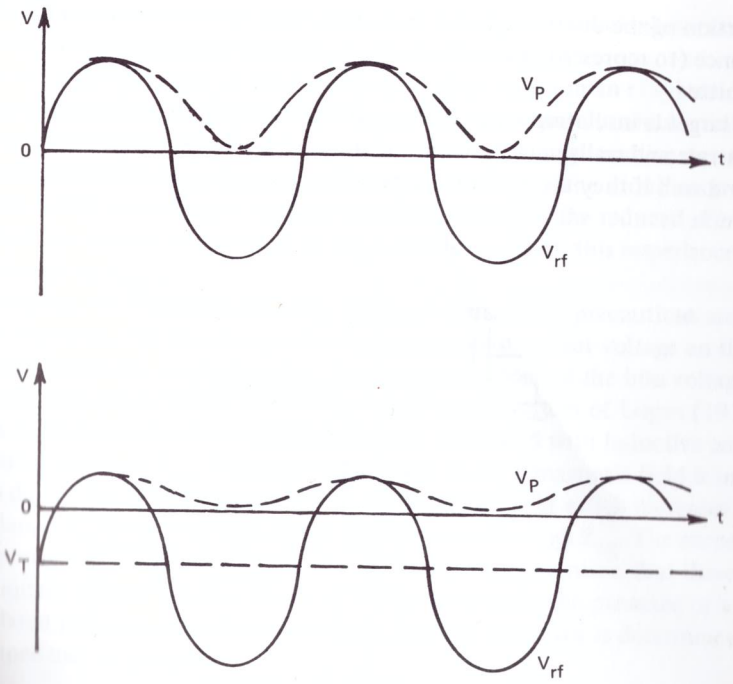

Figure 5-23. Voltage V_{rf} across rf system
(a) Symmetrical system, $V_T = 0$
(b) Asymmetric system, V_T is negative (Christensen and Brunot 1973)

EQUIVALENT CIRCUITS OF RF DISCHARGES

It is often convenient to represent an rf discharge system by an electrical equivalent circuit. This has been done by Koenig and Maissel (1970), and by many others. Although the details of the various proposals differ, the basic features are as shown in Figure 5-24a.

The elements Z_t, Z_s and Z_w are the impedances of the sheaths at the target, substrate and walls, respectively. The detail of these sheath impedances is shown in Figure 5-24b. The sheath is primarily capacitive due to the positive ion space charge in the sheath and the compensating negative surface charge on the adjacent surface (target or deposited film). The diode allows for the asymmetry of the ion and electron currents. The resistors r and R are often omitted; r limits the electron current and will be small, whereas R allows for power dissipation due to collisions, and will be very large at very low pressures, decreasing (more power dissipation) at higher pressures. The final element Z_g represents the rele-

vant portion of the distributed glow impedance; this is sometimes simplified to a resistance (to represent power losses due to inelastic collisions) and sometimes even omitted.

If the target is insulating, then the capacitances of the target and the films on the substrate and walls must be included, as must the capacitances of the substrate and wall if they are not conducting. The target-ground shield capacitance

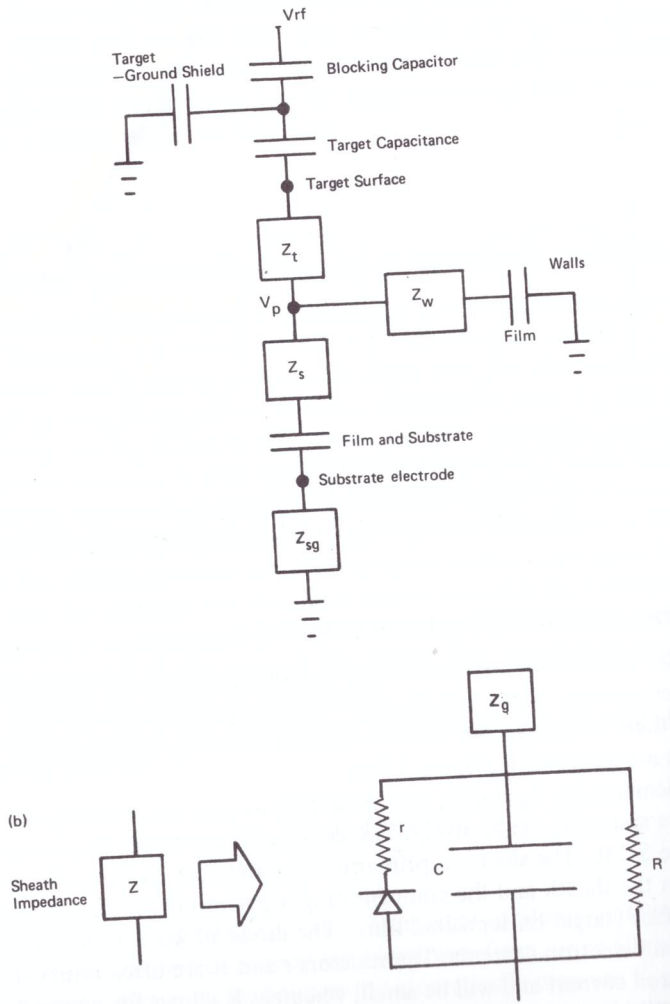

Figure 5-24. Equivalent circuit of an rf discharge

has an effect on the reactive current flowing through the matching network and therefore has an effect on the power losses in the network.

It is not a trivial matter to electrically ground an object in an rf system; even a straight piece of conducting wire will have some inductance L which can lead to sizeable voltage drops along the wire because of the large reactive currents involved. With increasing frequency, the reactance ωL of the inductance will increase whilst its resistance will also increase because of the reduced *skin depth* to which the current is confined. In the equivalent circuit, this impedance is represented by Z_{sg}.

Sometimes one wishes to minimize Z_{sg}, and then special precautions are taken. However, one can also positively control the dc offset voltage on the substrate holder by controlling Z_{sg}, for example to control the bias voltage in a sputtering system. This is done in the *tuned anode* system of Logan (1970). Figure 5-25 shows the dc substrate potentials developed with inductive and capacitive values of Z_{sg}. The larger effect with an axial magnetic field is interpreted as due to the constraining effect of the magnetic field which increases the impedance Z_w to the wall and forces more current through Z_{sg}. The success of this approach is a further confirmation of the earlier contention that there is no uniquely defined floating potential on an insulator in the presence of a modulated plasma potential, and that the 'floating' potential is determined by the impedance to ground.

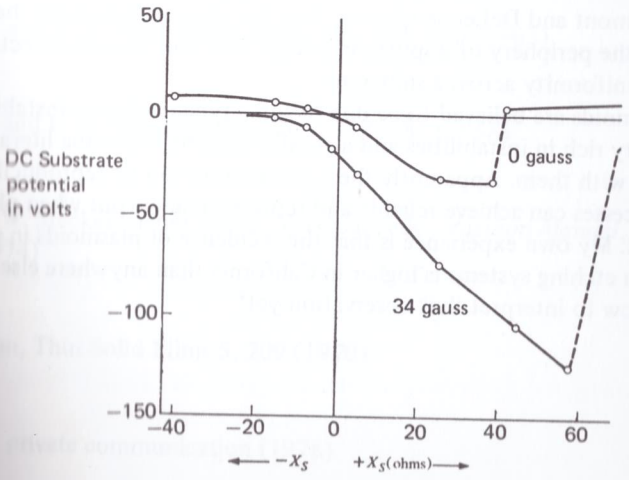

Figure 5-25. Substrate bias dependence on substrate tuning impedance. Frequency 13.56 Mhz, power density 3.9 W/cm², argon pressure 15 mtorr (Logan 1970)

PLASMOIDS

There are certain subjects that rarely are discussed in glow discharge articles, but are common knowledge amongst folks who play regularly with these systems. Such subjects include things such as initiating a discharge with a transient burst of pressure or voltage, things that seem too obvious to mention (but only in retrospect!). Another common observation is of *plasmoids*, and these seem not to be discussed because of lack of comprehension, though I might be wrong. A plasmoid is generally described as a volume of more intense glow than its surroundings. Some plasmoids are easy to explain, including those inside hollow cylindrical regions such as entry ports in a chamber, where the enhanced glow is due to a *hollow cathode effect*: the normal ejection of electrons by the sheath field around the inside of a cylinder causes an enhanced electron density along the axis and in the glow. But more mysterious are those plasmoids that occur in the body of the glow. They sometimes occur in groups symmetrically arranged about the axis of the discharge at about the target radius, or sometimes as a single plasmoid similarly located, and are either stationary or rotate in either direction, with continuous motion or regular discrete jumps.

The only reference to these plasmoids in the sputtering literature that I know of, is by Lamont and DeLeone (1970). They compare the form of the plasmoids to the spokes (1, 2, 6 and 8) of a wagon wheel, either stationary or rotating. They report that plasmoids were observed and named as early as 1930, and briefly mention some mechanisms and give some further references. I haven't studied these and can't elucidate the proposed mechanisms. Of practical import, Lamont and DeLeone propose that the plasmoids increase the current density at the periphery of a sputtering target and thus have an effect on the thickness uniformity across a substrate.

The plasmoids are believed to be due to some type of plasma instability; plasmas are very rich in instabilities and a goodly amount of plasma literature is concerned with them. Apparently these instabilities can be reproducible, though, and rf processes can achieve reliable and reproducible output when plasmoids are present. My own experience is that the incidence of plasmoids in sputtering and plasma etching systems is higher in California than anywhere else, but I am not sure how to interpret that observation yet!

REFERENCES

G. S. Anderson, W. N. Mayer, and G. K. Wehner, J. Appl. Phys. **33**, 2991 (1962)

F. Bresnock, Proc. IEEE Intern. Conf. on Plasma Science, Montreal (1979)

H. S. Butler and G. S. Kino, Phys. Fluids **6**, 1346 (1963)

B. N. Chapman, Proc. MRC Conference on Sputtering, Brighton (1969)

B. N. Chapman, previously unpublished results (1975)

O. Christensen and M. Brunot, Le Vide, Les Couches Minces **165**, 37 (1973)

J. W. Coburn and Eric Kay, J. Appl. Phys. **43**, 4965 (1972)

W. D. Davis and T. A. Vanderslice, Phys. Rev. **131**, 219 (1963)

A. J. Hatch and H. B. Williams, Phys. Rev. **112**, 681 (1958)

L. Holland, W. Steckelmacher, and J. Yarwood, eds., *Vacuum Manual*, Spon, London (1974)

G. N. Jackson, Thin Solid Films **5**, 209 (1970)

J. M. Keller, private communication (1978)

J. M. Keller and W. B. Pennebaker, IBM J. Res. Develop. **23**, 3 (1979)

H. R. Koenig and L. I. Maissel, IBM J. Res. Develop. **14**, 168 (1970)

H. R. Koenig, U.S. Patent 3 661 761 (1972)

L. T. Lamont Jr. and J. J. DeLeone Jr., J. Vac. Sci. Tech. **7**, 155 (1970)

J. S. Logan, N. M. Mazza, and P. D. Davidse, J. Vac. Sci. Tech. **6**, 120 (1969)

J. S. Logan, IBM J. Res. Develop. **14**, 172 (1970)

A. D. MacDonald and S. J. Tetenbaum, in *Gaseous Electronics*, Vol. 1, ed. Merle N. Hirsh and H. J. Oskam, Academic Press, New York and London (1978)

L. I. Maissel, in *Handbook of Thin Film Technology*, ed. L. I . Maissel and R. Glang, McGraw Hill (1970)

R. B. McDowell, Solid State Tech., p. 23, February (1969)

W. B. Pennebaker, IBM J. Res. Develop. **23**, 16 (1979)

R. T. C. Tsui, Phys. Rev. **168**, 107 (1968)

S. Vacquie, J. Bacri and G. Serrot, Comptes Rendu **266**, 387 (1968)

J. L. Vossen and J. J. O'Neill Jr., J. Vac. Sci. Tech. **12**, 1052 (1975)

J. L. Vossen, J. Electrochem. Soc. **126**, 319 (1979)

G. K. Wehner, Adv. in Electronics and Electron Physics **VII**, 253 (1955)